

Vision-Language Models can Identify Distracted Driver Behavior from Naturalistic Videos

Md Zahid Hasan, Jiajing Chen, Jiyang Wang, Mohammed Shaiqur Rahman, Ameya Joshi, Senem Velipasalar, Chinmay Hegde, Anuj Sharma, Soumik Sarkar

Abstract—Recognizing the activities causing distraction in real-world driving scenarios is critical for ensuring the safety and reliability of both drivers and pedestrians on the roadways. Conventional computer vision techniques are typically data-intensive and require a large volume of annotated training data to detect and classify various distracted driving behaviors, thereby limiting their generalization ability, efficiency and scalability. We aim to develop a generalized framework that showcases robust performance with access to limited or no annotated training data. Recently, vision-language models have offered large-scale visual-textual pretraining that can be adapted to task-specific learning like distracted driving activity recognition. Vision-language pretraining models like CLIP have shown significant promise in learning natural language-guided visual representations. This paper proposes a CLIP-based driver activity recognition approach that identifies driver distraction from naturalistic driving images and videos. CLIP’s vision embedding offers zero-shot transfer and task-based finetuning, which can classify distracted activities from naturalistic driving video. Our results show that this framework offers state-of-the-art performance on zero-shot transfer, finetuning and video-based models for predicting the driver’s state on four public datasets. We propose frame-based and video-based frameworks developed on top of the CLIP’s visual representation for distracted driving detection and classification tasks and report the results. Our code is available at <https://github.com/zahid-isu/DriveCLIP>

Index Terms—Distracted driving, Computer vision, CLIP, Vision-language model, Zero-shot transfer, Embedding

I. INTRODUCTION

Distracted driving accounts for almost 10% of all fatalities on U.S. roads. Although cell phone usage is often synonymous with distracted driving, the problem is broader. The Center for Disease Control and Prevention (CDC) identifies three forms of distraction: i) visual distraction, where the driver takes their eyes away from the road. This can be due to several reasons, such as looking at the GPS, Billboard, etc.; ii) manual distraction, where the driver takes their hands off

of the steering wheel; and iii) cognitive distraction, where the driver takes their mind off the driving task, which can be due to singing, talking etc. The association of crashes with distracted behavior is underreported. Verifying the distraction in the post-crash investigation is difficult, and the driver at fault might not disclose this information voluntarily. Contrary to the numbers reported in crash analysis, Naturalistic Driving Data analysis by Dingus et al. [1] reported that almost 90% of their studied 905 crashes, which resulted in injury or property damage, can be attributed to driver-related factors (i.e., error, impairment, fatigue, and distraction). Naturalistic driving study (NDS) research involves observing drivers in real-world settings using unobtrusive instruments fitted to their vehicles. These studies cover drivers’ daily driving activity for a few months to years. With low-cost sensors and robust data handling infrastructure, NDS research is now easier to implement and has paved the way to comprehensively understanding the occurrence of driving events and driver responses in a natural environment. In most recent studies, such analysis has required humans to annotate driver distraction manually. The manual approach is useful but very time-consuming and significantly increases the analysis time. This study aims to reliably and efficiently identify distracted driving actions by drivers from naturalistic driving videos.

With the significant advances in deep learning and computer vision, there has been a considerable surge in video analytics for the classification of distracted driving. In recent studies, convolutional neural networks (CNN) have been widely employed for video-based distracted driving detection. For instance, Moslemi et al. [2] proposed a 3D CNN model for distracted driving detection using a dataset composed of videos captured in a naturalistic driving study. This model was designed to learn spatiotemporal features from video sequences, thus allowing it to capture not only the appearance of distracted behaviors but also their temporal dynamics. However, this type of model often requires large amounts of labeled training data, which is both time-consuming and costly to collect and annotate. Therefore, researchers have recently begun to investigate unsupervised [3] and semi-supervised [4] learning techniques. For instance, Xie et al. [5] introduced a semi-supervised learning method for distracted driving detection, wherein they combined labeled and unlabeled data to train their deep learning model.

The recent development of vision-language multimodal pretraining frameworks showcases promising potential across diverse applications [6]–[9]. These pretraining frameworks employ a multi-modal contrastive-loss (see CLIP [10]), which

M.Z. Hasan, M.S. Rahman, A. Sharma, and S. Sarkar are with Iowa State University, Ames, IA-50010, e-mail: {zahid, shaiqur, anuj, soumiks}@iastate.edu

J.Chen, J. Wang and S. Velipasalar are with the Department of Electrical Engineering and Computer Science, Syracuse University, Syracuse, NY-13244, e-mail: {jchen152, jwang127, svelipasg}@syr.edu

A. Joshi and C. Hegde are with the Department of Electrical and Computer Engineering, Brooklyn, NY-11201, e-mail: {ameya.joshi, chinmay.h}@nyu.edu

This material is based upon work supported by the Federal Highway Administration Exploratory Advanced Research Program under Agreement No. 693JJ31950022. Any opinions, findings, and conclusions or recommendations expressed in this publication are those of the Author(s) and do not necessarily reflect the view of the Federal Highway Administration.

Manuscript received June 22, 2023; revised 4 January 2024.

arXiv:2306.10159v3 [cs.CV] 4 Jan 2024

paves the way for creating robust embeddings encompassing both text and vision tasks concurrently. This approach allowed several domains to use an almost zero-shot approach for tasks, such as object classification and object detection from images [10]–[13]. The study presented in this paper leverages CLIP’s vision and language embeddings for the specific task of distracted driving action recognition.

Distracted driving action recognition involves analyzing video data captured from a camera positioned inside the car, which records extensive time frames of driver behavior. The goal is to utilize this video data to determine whether the driver is distracted. Intuitively, one might consider training a video-text model from the ground up for this task. However, directly training such a model is impractical due to the need for large-scale video-text training data and considerable GPU resources. A more viable approach is to adapt pre-existing language-image models to the video domain [14]–[16]. Several recent studies have investigated strategies for transferring knowledge from these pretrained language-image models to other downstream tasks [12], [17]–[20].

Our proposed method benefits from key aspects of the pretrained CLIP model [10] and provides two main advantages. The first advantage is its ability to utilize zero-shot transfer, obviating the need for intensive training. This feature enhances scalability and feasibility, allowing for a natural language-supervised understanding of video activities rather than relying exclusively on traditional supervised approaches. Unlike conventional computer vision methods, which tend to memorize human-annotated labels or features often found non-transferable, this model generally exhibits superior performance across diverse datasets rather than constrained to a specific dataset. The second advantage of the proposed method is the potential to further finetune the visual representation with minimal annotations and training, thereby enhancing the system’s overall performance. In addition, it allows us to assess the generalizability and robustness of the finetuned models in diverse real-world settings.

In summary, the key contributions of this work include the following:

- 1) We introduce and explore the performance of various vision-language-based frameworks (adapted from [10]) for distracted driving action recognition tasks with minimum training. Moreover, we propose a unique validation method named ‘leaving a set of driver out’, which involves subject-wise separation during training to prevent overfitting to specific driver characteristics. It also tests the model’s generalizability to previously unseen driver behaviors.
- 2) We present both frame-based and video-based models and show that including temporal information in the existing vision-language models offers superior performance on several distracted driving datasets. Moreover, we execute an exhaustive fine-tuning with extensive hyperparameter tuning across multiple datasets to achieve the optimized performance on our proposed models. This confirms the models’ effectiveness in recognizing driver distractions under a variety of real-world conditions.

- 3) We perform an in-depth analysis of the models’ performance across different datasets and various experimental settings. We demonstrate the model’s robustness and strong generalization ability by maintaining high-performance levels even with reduced training data sizes. These attributes underscore the potential for deploying our models in real-world scenarios where training data may be limited.

In this study, we have developed and tested four unique frameworks on four distinct datasets that are tailored specifically for analyzing distracted driving behavior. These frameworks include both frame-based and video-based models. The rest of this paper is organized as follows: Section II provides a review of relevant research on distracted driving action recognition, highlighting key contributions as well as gaps that our study aims to address. Section III introduces the details of our methods. Section IV provides details about the datasets and the experimental setup for each framework. Section V presents the results of the performance evaluation of the proposed frameworks, performance comparison with existing models for distracted driving, an investigation into the impact of different real-world settings on the model performance and an ablation study. The paper concludes in Section VI.

II. RELATED WORK

In recent years, the area of driver action recognition and behavior analysis has attracted significant research interest. Various methods have been proposed including -

A. Machine Learning-based Techniques

Prior to recent advances in computer vision, traditional machine learning approaches primarily relied on manually selecting key features and pairing them with a classifier [21]. Features were collected from the driver’s hand, head-pose, face, body-pose, eye gaze [22]–[27] or sensors [28], [29]. The choice for common classifier includes SVM [30], HMM [31], random forest [32], KNN [33] and so on. However, the major limitation of these methods is that the manual feature selection lacks generalization, making it challenging to apply them effectively across diverse driving scenarios [34]. Many of these techniques are specifically tailored to certain datasets, which lack broad applicability due to the lack of end-to-end training on large-scale data.

B. Supervised Learning-based Techniques

The emergence of camera sensors and advancements in Convolutional Neural Networks (CNNs) have significantly influenced the field of computer vision and driver observation. As a result, a significant portion of the current methodologies depended on various supervised CNN models [35]–[37] for extracting important features from image and video content. Some CNN-based frameworks gather features from facial recognition [38], optical flow [39], and body posture assessment [40] for distraction action recognition. Some of the most common CNN backbones used in literature are VGG16 [41], ResNet50 [42], AlexNet [43], Inception-v3 [44], MobileNet-v2 [45], ShuffleNet-v2 [46] etc. Various CNN approaches are

employed based on the availability of dimensions (2D/3D), modalities (RGB, IR, Depth, [35], [36]), camera views (front, side etc) of datasets and ensemble techniques [47]. Traditional video-based action recognition CNN models often evolve from image-based 2D CNN models, adapting to incorporate the temporal aspect of videos. Strategies for integrating the temporal dimension include using 2D CNNs on multiple frames or 3D CNNs on video clips [48], [49]. However, these supervised CNN-based approaches require vast amounts of labeled data for training, making the process resource-intensive. This heavy reliance on extensive labeled data poses a significant challenge and can limit their generalization capabilities [3]. Furthermore, while 3D CNNs can learn temporal features from video sequences, their implementation is often limited by high computational requirements and real-world challenges in processing naturalistic videos [48], [50], [51]. Another technique that is commonly adopted involves ensembling multiple CNN networks [52]–[54]. Here, each CNN works as a unique feature extractor. Finally, they are incorporated into a weighted ensemble to yield a comprehensive global feature. In addition, there are methods that adopt feature-level fusion [48], [55], [56]. These methods separately learn from RGB appearance and time-based features and later combine the learned features.

C. Weakly-Supervised Learning-based Techniques

The landscape of distracted action recognition is increasingly being shaped by Vision Transformer (ViT)-based techniques [57]–[60], which have started to dominate in video action recognition recently. A ViT-based, weakly supervised contrastive (W-SupCon) learning approach is proposed in [4], where it quantifies distracted behaviors by measuring their deviation from the normal driving representations. A key limitation of this study is the challenge of distinguishing high-risk driving behaviors from normal ones due to their similar physical movements indicating limited generalization.

D. Unsupervised Learning-based Techniques

A multilayer perceptron-based unsupervised model is proposed in [3] where a ResNet50 [42] backbone is trained for enhanced feature extraction. However, this approach’s generalizability is limited, having been tested on only one dataset without large-scale validation.

The recent progress in vision-language pretraining approaches [12], [19], [61] has demonstrated improved performance in tasks related to video action recognition tasks. These models are developed on a widely used vision-language model named CLIP [10]. For video-based CLIP training, Miech et al. [62] introduce a large dataset referred to as HowTo100M. Additionally, for learning the visual-semantic joint embedding, Mithun et al. [63] propose a two-stage approach that leverages web images and corresponding tags. Dong et al. [64] attempt to solve the challenging problem of zero example video retrieval using textual features. Therefore, different methods have been developed to effectively learn from and utilize visual and textual data for tasks and visual-semantic joint embedding, which underlines the potential of integrating visual and textual

data in developing advanced models. While the CNN and ViT-based models exhibit satisfactory results on specific datasets, their effectiveness is significantly tied to large-scale data and substantial efforts for data annotation. Additionally, the training of these models is often geared towards mapping predefined categories, which impedes their ability to learn adaptable visual features on new data. Therefore, rather than confining the learning to specific visual features within a single modality framework, learning from natural language supervision could provide increased adaptability and wider applicability [10]. Our method leverages the pretrained CLIP model to offer two significant benefits. Firstly, it enables zero-shot transfer, eliminating the requirement for extensive dataset-specific training. Secondly, it allows further finetuning of visual representations with only a small amount of training data. Moreover, our approach addresses the overfitting issue encountered in previous studies where subject-level separation in training and testing sets was not maintained. We discuss this step in detail in section III

III. METHODOLOGY

The primary objective of this work is to understand distracted driving behaviors captured from in-vehicle video footage and build an effective driver monitoring system. While distractions during driving can span a variety of situations, we predominantly focus on actions that disrupt the driver’s attention from the primary task of safely operating the vehicle on the road. In addition, we only focus on a single distracted action that occurred for a certain duration and consider the action as a distracted event. We also assume that there are no multiple distracted events occurring simultaneously. Examples of distracted events are talking on the phone, reaching behind, or drinking water while driving. Visual data associated with distracted driving can present several complications in detecting distracted driving, including low-quality video data and the extensive human effort required to annotate videos for training supervised models. Furthermore, without a large volume of annotated visual data, training a high-performance supervised network is impossible. Therefore, we investigate to create a generalized framework that performs well without a strict reliance on labeled data or with only limited labeled data. To achieve this, we propose to leverage a contrastive vision-language pretraining framework designed to tackle these challenges with minimal annotated data. Moreover, we pay special attention to how our experiments were conducted, ensuring a robust and generalizable testing strategy. In real-world scenarios, the model will be expected to generalize its learning to new and unseen drivers. Therefore, we employed two combined methods: 1) subject-wise separation - ‘*leaving a set of driver out*’ method where we separate out a unique set of driver samples only for testing. 2) subject-wise cross-validation - *k-fold cross-validation* method where we implement *k-fold cross-validation* technique individually to each driver set. For the first approach, the test split drivers’ data are never presented to the model during its training phase. It ensures that the model can make inferences fully on unseen data during testing. These two methods ensure

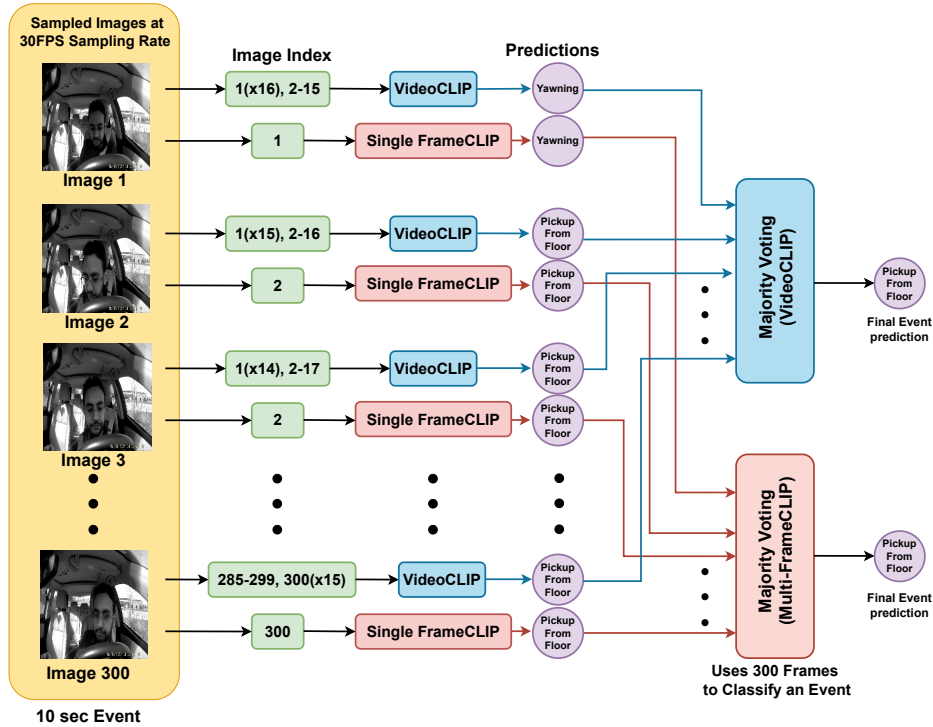


Fig. 1. An overview of the image-based and video-based CLIP frameworks. The yellow box shows the sampled frames from a 10-second event, i.e., a total of 300 frames at a rate of 30 frames per second. These frames are sampled from raw data (as depicted in Fig. 3). The VideoCLIP model uses 30 consecutive frames to form a short video clip as input, while the Single-frameCLIP model takes a single frame at a time. For the first sampled frame, the VideoCLIP generates a 30-frame video clip by repeating Image-1 sixteen times and including Images 2 to 15 (a total of 30 frames in the green box). The SingleframeCLIP model only uses Image-1 as its first input. This process continues for each subsequent frame. Finally, predictions for an entire event are made by calculating the majority vote from all individual frame predictions. Note that the Multi-frameCLIP applies majority voting on SingleframeCLIP’s predictions to get the final event prediction.

zero overlapping between training and testing splits and zero memorizing across all the runs we conducted. The average accuracy obtained from all the k -fold results is reported as the final accuracy of our frameworks. This process allows us to accurately assess the overall performance of our proposed distracted driving models across all the datasets.

Furthermore, we recognize the significance of addressing multiple distracted driver behaviors occurring simultaneously or alternately. Our observations have revealed that the effectiveness of handling such scenarios is dependent on the specific datasets used and the formulation of prompts. It’s essential to underscore that dealing with multiple distracted behaviors is indeed a complex challenge within the scope of this problem. While our current framework has not been specifically tested on scenarios involving multiple distracted behaviors, we firmly believe that, with the availability of appropriate datasets and prompt customization, our framework can be adapted to successfully detect and analyze such situations. We acknowledge that this aspect of the problem requires further research and exploration.

A. Proposed Frameworks

We fundamentally propose two methodologies: (i) frame-based models (Zero-shotCLIP, Single-frameCLIP, and Multi-frameCLIP) and (ii) a video-based model (VideoCLIP). An overview of these frameworks is provided in Fig. 1. CLIP [10] is a popular vision-language model. It is proficient in most

visual understanding tasks since it was trained on a large variety (around 400 million) of image-text pairs from the web.

1) Frame-based models

The frame-based models operate by taking inputs similar to the original CLIP model and making predictions on distracted actions. As shown in Fig. 2, the model projects the input image and text pairs into a multi-modal latent space and minimizes a contrastive loss, which enables it to learn meaningful and useful visual and textual representations. Therefore, the base model can be fine-tuned for task-specific learning. Given its ability to be instructed by natural language for a broad range of downstream tasks, such as video question answering and

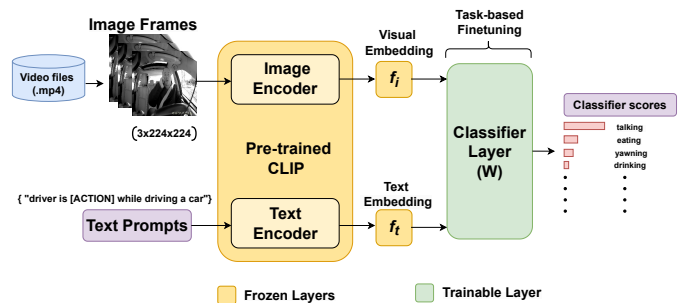


Fig. 2. The proposed multimodal Single-frameCLIP framework exploits the pretrained CLIP architecture to extract vision-text semantic information.

understanding actions from video, we develop our distracted driving analysis framework based on this model. A great advantage of using a pre-trained network over other strategies is the ability to utilize the pre-existing visual representation of the language prompt, offering the zero-shot transfer. In this work, we initially leverage CLIP’s pre-trained visual embedding for zero-shot transfer on distracted driving datasets and categorize the distracted action classes without any additional training. Following this, we fine-tune a linear classifier layer built upon the original pre-trained CLIP model. The yellow block shown in Fig. 2 represents the frozen layers. We add the green block positioned on top of the yellow layers, which represents the trainable layer. This task-based fine-tuning green block involves training a straightforward classifier layer using the pre-existing embeddings from the frozen layers for a specific task. In our case, this task is to classify distracted driving actions from visual data. We evaluate the performance of the whole framework on corresponding distracted driving datasets. As per the primary model [10], we implement six CLIP visual backbones- ViT-L/14, ViT-L/14@336px, ViT-B/16, ViT-B/32, RN101 and assess each of their performance individually.

The Zero-shotCLIP, Single-frameCLIP and Multi-frameCLIP frameworks have input $I \in \mathbb{R}^{3 \times H \times W}$ where I , H , and W represent the input image, image height and image width, respectively. The Zero-shotCLIP makes predictions on raw frames without requiring any training. The key difference between the other two frameworks is that Single-frameCLIP makes predictions looking at a single frame and the Multi-frameCLIP makes predictions on a stack of frames conducting a majority vote at the classification layer. For both frame-based and video-based CLIP, all the layers up to the classifier layer were kept frozen and we only finetuned the last trainable (green) layer (shown in Fig. 2).

2) Video-based model

The VideoCLIP model has a similar structure to the frame-based model shown in Fig. 2, but uses a different CLIP visual encoder and model input. It utilizes a branch called S3D (separable 3D CNN) [5], a video processing backbone based on 3D-CNN, which takes a video $V \in \mathbb{R}^{S \times 3 \times H \times W}$ as input and encodes the video into a feature vector F . Here S , V , H , and W represent the number of frames, image height and image width, respectively. In our experiments, the number of frames S is set as 30, indicating that the VideoCLIP model uses 30 frames and synthesizes them into a short video clip. The rest of the training process is similar to the frame-based CLIP. In the training process, if the cosine similarity between the video feature and its corresponding text feature is high, the distance between their feature vectors is minimized. It should be highlighted that both the Multi-frameCLIP and VideoCLIP operate on successive frames, thereby capturing the temporal context of a given distracted action. A majority vote strategy is employed at the final stage by both frameworks. The key difference between these two models is illustrated in Fig. 1, with a comprehensive discussion provided in Section IV.

Fig. 3 shows the overall sampling procedure that we follow for our experiments. The blue block on the left shows some raw frames from the original video, which has a frame rate

of 30 frames per second (FPS). The yellow blocks show the sampled frames at corresponding sampling rates. Due to the CLIP network’s limitations in processing numerous frames simultaneously, we sample the frames from the video data at various sampling rates and create a 30-frame-long video clip to feed into the VideoCLIP network. From Fig. 3, it could be observed that when the sampling rate is high, such as 20 FPS, the consecutive frames exhibit little semantic differences, and the video snippet (created from the 30 frames) covers less time duration. In contrast, if the sampling rate is low, the video snippet could span a longer time duration, with greater semantic differences between two consecutive frames. We perform a series of experiments to determine the best sampling rate for the video-based framework, discussed in Section IV, and the results of the experiments are explained in Section V.

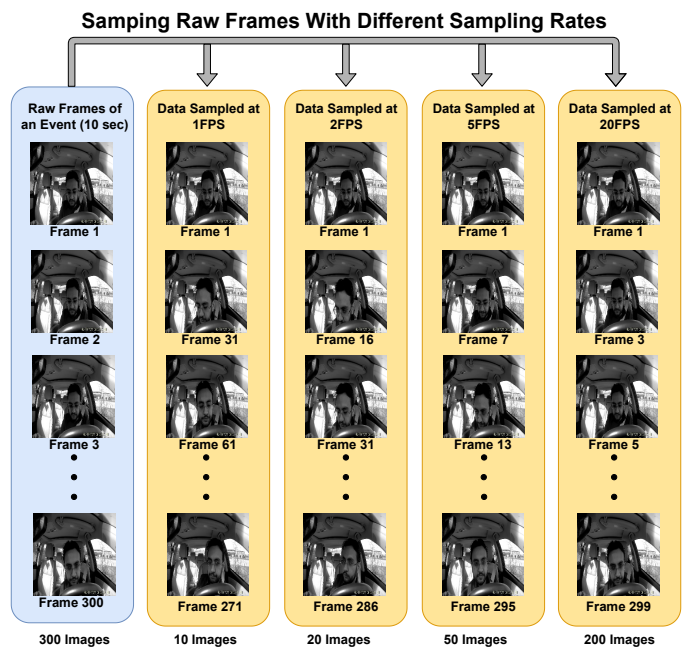


Fig. 3. The raw data is shown in the blue box, which contains 300 frames of an event lasting for 10 seconds. In other words, each second covers 30 frames. We sample frames with different sampling rates from the raw data, and the sampled data is shown in the yellow box. For example, when the sampling rate is two frames per second (FPS), we sample two images from 30 raw frames covered in each second. Since the raw data lasts for 10 seconds, we will have a total of 20 sampled images in the end.

IV. EXPERIMENTS

A. Dataset

The datasets used in our study are specifically chosen for their unique driver IDs or folders for each participant. This feature is crucial for conducting our ‘leave a set of driver out’ approach while testing. We evaluate our proposed frameworks on four distinct distracted driving datasets - DMD [35], SAM-DD [4], SynDD1 [65] and StateFarm [66]. These datasets serve as standard benchmarks for the analysis of distracted driving behavior, typically providing annotated images and videos that correspond to diverse distracted driving behaviors exhibited by participants. Each dataset comes with an

individual driverID (SAM-DD has separate folders for each participant) for each participant.

For our experiments, we utilize the driverIDs to separate out a specific set of drivers only for testing purposes, ensuring no overlapping between training and testing splits. Therefore, our framework does not get the chance to memorize the driver’s appearance and only focuses on distracted actions. We believe this is crucial for properly validating our algorithm’s effectiveness. This approach addresses the inaccuracies encountered in previous studies where such separation was not maintained. Moreover, to ensure consistency and reliability in our experimental approach, we executed all our experiments for all the proposed models with the same experimental settings across all the datasets we used. In addition, we assess the performance of our distracted driving models through a k -fold cross-validation approach executed on each driver set. Then, we calculate the average accuracy across all the k folds and report it as the final accuracy of the models. Moreover, we analyze the proposed frameworks’ performances for each dataset separately and report them in the subsequent sections.

B. SynDD1 Dataset

The SynDD1 dataset [65] is a recent addition to distracted driving datasets, offering insights into naturalistic distracted driving behaviors. The dataset includes videos of distracted driving events recorded by cabin cameras inside the vehicle. A total of 18 participants performed various in-car driving activities, which were recorded (as video) from three distinct camera angles - the dashboard camera, the rear-view mirror camera, and the right-side window camera. The videos have two types of annotation files - gaze activity and distracted activity. The first row of Fig. 4 shows some sample frames of distracted driving actions from the dashboard camera view. There are 18 driving activities performed by the participants, including ‘normal forward driving’, ‘drinking’, ‘phone call (right hand)’, ‘phone call (left hand)’, ‘eating’, ‘texting (right hand)’, ‘texting (left hand)’, ‘hair and makeup’, ‘reaching behind’, ‘adjusting control panel’, ‘pick up something from the floor (driver seat)’, ‘pick up something from the floor (passenger seat)’, ‘talking to the passenger at right’, ‘talking to the passenger at the backseat’, ‘yawning’, ‘hand on the head’, ‘singing’, ‘shaking or dancing’. Each video file comes with annotations, including action types, the start and end time of an action, the appearance of the participant and so on. Therefore, we have the start and end time of a particular distracted action and their corresponding time duration. Each distracted driving video has a frame rate of 30 FPS. Each frame has an RGB resolution of 1920x1080 pixels. For the purpose of this study, we consider the distracted behaviors of 14 drivers, thereby generating a more concise distracted driving dataset. For further generalization, we merge the similar action categories and consider eight distinct distracted actions shown in Table I. Fig. 5 shows the distribution of the distracted driving action duration (in seconds) across eight classes. The X-axis enumerates the eight specific distracted driving action categories, while the Y-axis represents the corresponding duration (sec) of these actions aggregated across all drivers.

The average action duration is approximately 18.692 seconds. The median and spread of the action duration suggest an almost uniform distribution. Consequently, the probability of a specific distracted driving action being more prevalent than others within the examined range is nearly zero. Therefore, the likelihood of occurrence for all durations of distracted driving actions is essentially equal. However, it is important to note that perfectly uniform distributions are rare to see in real-world scenarios, especially in studies related to human behavior.



Fig. 4. Sample dashboard camera frames from SynDD1 dataset- (a) drinking, (b) adjusting hair, (c) talking to phone (right hand); Statefarm dataset- (d) drinking, (e) adjusting hair, (f) talking to phone (left hand)

TABLE I
DISTRACTED DRIVING ACTION CATEGORIES FOR SYNDD1 DATASET

ID	distracted driving prompt description
0	driver is adjusting his or her hair while driving a car
1	driver is drinking water from a bottle while driving a car
2	driver is eating while driving a car
3	driver is picking something from the floor while driving a car
4	driver is reaching behind to the backseat while driving a car
5	driver is singing a song with music and smiling while driving
6	driver is talking to the phone on hand while driving a car
7	driver is yawning while driving a car

C. StateFarm Dataset

The StateFarm dataset [66] serves as a common dataset for distracted driving behavior analysis, providing only image (RGB) data. The images were captured from an in-cabin camera positioned on the right-side window, offering a right-side perspective of the driver, as (d), (e) and (f) of Fig. 4. Data were collected from 26 participants, and the total number of image frames is 22,424. Similar to the SynDD1 dataset, the StateFarm dataset includes unique driver IDs for each participant, which enables us to perform the ‘leave a set of driver out’ step and driver-level k-fold cross-validation. However, it does not provide information on the action duration, start, or end times of actions as the labels pertain only to image frames. There are ten distracted driving activity categories in total- ‘normal driving’, ‘texting (right hand)’, ‘talking on the phone

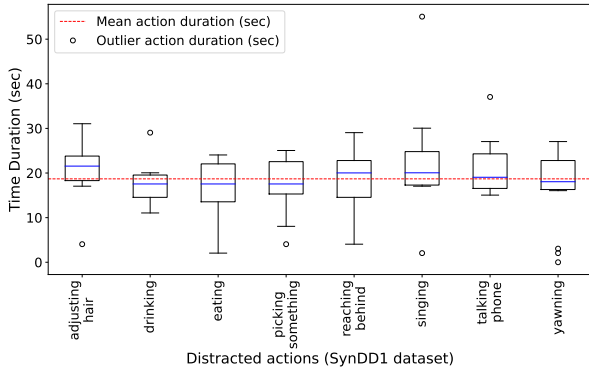


Fig. 5. The distribution of the time duration (sec) across eight distracted driving actions from the SynDD1 dataset. The mean action duration is 18.692 seconds. The median and spread of the action duration suggest an almost uniform distribution, demonstrating a balance in the action categories we use.

(right hand), ‘texting (left hand)’, ‘talking on the phone (left hand)’, ‘operating the radio’, ‘drinking’, ‘reaching behind’, ‘hair and makeup’, ‘talking to a passenger’. The images have a resolution of (640,480,3). We consider all the drivers and ten action categories for our experimental analysis.

D. DMD Dataset

The Driver Monitoring Dataset (DMD) is a specialized dataset [35] designed to facilitate research in driver distraction and behavior recognition. This dataset captures various aspects of driver activity in 37 participants- focusing on distraction, drowsiness, hand movements, and gaze direction. This dataset offers RGB images (up to 1920x1080 pixels), depth data, and corresponding metadata with ten distraction categories. The data was recorded in two different environments - outdoors in a real car and indoors in a driving simulator. There are ten distracted driving actions, including ‘drinking water’, ‘adjusting hair and makeup’, ‘talking to the phone on right hand’, ‘adjusting radio’, ‘reaching to the backseat’, ‘reaching side’, ‘driving safely’, ‘talking to the passenger’, ‘texting on the phone with right hand’ and ‘yawning’. We implemented a 7-fold cross-validation on the ten distraction classes with 78917 samples for each fold and 552419 samples in total for all the folds. In addition, we performed the ‘leave a set of drivers out’ method using the provided driver IDs within the 7-fold cross-validation to evaluate our model performance.

E. SAM-DD Dataset

The Singapore AutoManNTU distracted driving (SAM-DD) dataset [4] is a comprehensive dataset for intelligent driving research. It includes image data from 42 participants (34 males, 8 females) of diverse ages and driving experiences. It features 51,175 samples across front and side camera views, encompassing both RGB and Depth image modes. The dataset includes ten distinct distraction classes with nine physically distracted behaviors - ‘drinking’, ‘talking’, ‘texting’, ‘touching hair’, ‘adjusting glasses’, ‘reaching behind’, and a fatigue-related behavior (head dropping). The high resolution (1200x900 pixels) RGB data makes it suitable for developing

learning-based models in various driving environments and driver state-related applications. Both the DMD and SAM-DD are large datasets in terms of distracted class, number of samples per class and number of drivers. To ensure consistency and reliability in our experimental approach, we executed our proposed models with the same experimental settings for all the datasets.

F. Experiment Setup - ZeroshotCLIP and Single-frameCLIP

Our overall approach is depicted in Fig. 2. First, we explore the zero-shot transfer capability of the CLIP model on distracted driving data in the Zero-shotCLIP framework. Then, we explore the task-based finetuning route to evaluate the “task learning capability” of our proposed Single-frameCLIP framework. For the Zero-shotCLIP experiment, there is no training associated, and we simply predict the class-level confidence score of the pre-trained CLIP model on raw image frames (224x224x3). Next, we assess the representation learning capability of the pre-trained CLIP model on the distracted driving datasets in the Single-frameCLIP framework. We add an extra linear classifier layer on top of the pre-trained CLIP model architecture and train the single layer on distracted driving datasets. For training the linear classifier (see CLIP [10]), we use image frames of input size (224x224x3) collected from the four datasets. We utilize a batch size of 100 and a learning rate of 0.001. While training the Single-frameCLIP, we kept the pre-trained layers frozen and updated only the final layer based on the cross-entropy loss. Fig. 1 provides a visual representation of this approach, which generates predictions on a frame-by-frame basis. To illustrate this process, let’s consider a 10-second event sampled at a rate of 30 frames per second with a total of 300 frames (depicted in Fig. 1 by the yellow box). For each of these frames, the Single-frameCLIP model generates a prediction, beginning with the first frame (Image-1) and subsequently for each following frame (Image-2, Image-3, etc). In addition, based on the driverID, we perform an 8-fold cross-validation for the StateFarm datasets and a 7-fold cross-validation for the other three datasets. We report the average accuracy in Section V. Moreover, we experiment with various CLIP backbones (see CLIP [10]) and other hyperparameters. Notably, the original CLIP model employs semantic information in text labels rather than the traditional one-hot labels, which require providing a textual description or prompt for each action category. Therefore, we provide a full sentence as a prompt for describing the image frame of each action class instead of a single word. The prompt descriptions for the SynDD1 dataset are shown in Table I. As reported in [10], we consider manually fine-tuning and rephrasing the prompt sentences for our experiments, an area that can be further optimized in future work.

G. Experiment Setup - Multi-frameCLIP

The Multi-frameCLIP framework is specifically designed to analyze sequences of consecutive frames from distracted driving videos. This approach extends upon the Single-frameCLIP, concluding with an additional majority voting step applied

across consecutive frames to generate the final event prediction. The majority voting method allows our framework to make a single prediction on a particular action event. During the first step of training, this framework is provided with the frames between the start and end times of a specific action within the video footage. Following this, the Single-frameCLIP model is applied to each frame falling within these timestamps, providing individual predictions for each frame. A majority voting method is then employed to produce a final prediction. If this prediction aligns with the ground truth action label for that segment of the video, it is considered a correct prediction. This entire process is visually represented in Fig. 1. From the raw video data, we sample frames at varying rates (as depicted in Fig. 3). Let’s consider a 10-second event containing 300 frames captured at a rate of 30 FPS (shown by the yellow box). The Single-frameCLIP model is employed to make predictions for each of these frames, starting with the first frame (Image-1) and then sequentially progressing (Image-2, Image-3, and so on). Finally, a majority vote among all the individual frame predictions is taken to make a final prediction for the entire 10-second event in the video. This method allows Multi-frameCLIP to extend Single-frameCLIP’s capability by incorporating a temporal understanding of the events in a video clip. To ensure robust results, we conducted cross-validation experiments with sampling rates of 1, 2, 5, 20, and 0.5 frames per second.

H. Experiment Setup - VideoCLIP

The VideoCLIP is an adaptation of the frame-based CLIP model. It incorporates a 3D Convolutional Neural Network (CNN) backbone specifically designed for video processing. For additional information, readers can refer to [67]. The key difference in this model is its consideration of the temporal information of video data when making a prediction. When the model needs to make a prediction about a particular frame, it does not just look at that single frame. Instead, it combines 14 frames that come before and 15 frames that come after a particular target frame to form a small video footage. A total of 30 frames (including the target frame) are used together for prediction. This video piece is fed into the pre-trained CLIP backbone and a majority voting step is conducted to produce the final prediction. Fig. 1 shows an overview of the VideoCLIP model pipeline. This technique enables the model to consider not only the content of the targeted frame but also the preceding and subsequent frames. In this way, the network can perform classification with more complete temporal information. In this experiment, the learning rate and batch size are set as 0.0003 and 5, respectively, and Adam [68] optimizer is used. We followed the ‘leave a set of driver out’ method as before and split the drivers into two non-overlapping sets (training and testing) to evaluate the performance of never-before-seen drivers. Finally, we perform a 7-fold cross-validation on the splits with sampling rates of 1,2,5 and 20 frames per second.

I. Experiment Setup for CLIP vs. Other Models

For performance comparison, we further trained several mainstream CNN backbones, which are commonly used for

distracted driving recognition. For this experiment, we considered five different backbones - AlexNet [43], VGG16 [41], MobileNet-v2 [45], ResNet18 and ResNet50 [42], and implemented them on the frames sampled from the video data. We used the ImageNet pre-trained weights and fine-tuned the models with a learning rate of 0.001 and a batch size of 64. We used Adam [68] as the optimizer. We report the experimental results and outcome of our observation in Section V.

V. RESULTS

A. Performance of the Proposed CLIP-based Frameworks

We present the performance summary of various CLIP-based frameworks on the four distracted driving datasets in Table II. The VideoCLIP model with an optimal hyperparameter setting demonstrated the most superior performance with a Top-1 accuracy of 81.85%, 98.44% and 97.86% on SynDD1, DMD and SAM-DD datasets, respectively. This was followed by the Multi-frameCLIP framework with an optimal hyperparameter setting. Single-frameCLIP and Zero-shotCLIP reported lower Top-1 accuracies on the SynDD1 dataset compared to the Statefarm dataset.

TABLE II
PERFORMANCE SUMMARY OF CLIP-BASED
FRAMEWORKS ON DISTRACTED DRIVING DATASETS

Models (ours)	SynDD1		StateFarm		DMD		SAM-DD	
	Top-1	Top-3	Top-1	Top-3	Top-1	Top-3	Top-1	Top-3
Zero-shotCLIP	54.00	74.50	58.22	67.63	48.12	79.56	66.52	86.33
Single-frameCLIP	57.35	82.25	83.15	95.75	82.65	97.76	89.14	98.78
Multi-frameCLIP	70.36	75.38	N/A	N/A	93.39	95.74	89.14	90.27
VideoCLIP	81.85	91.96	N/A	N/A	98.44	99.80	97.86	99.76

On the StateFarm dataset, only Single-frameCLIP and Zero-shotCLIP were evaluated due to the absence of video data, which is a prerequisite for Multi-frameCLIP and VideoCLIP. Single-frameCLIP outperformed Zero-shotCLIP with optimal hyperparameter setting, achieving a Top-1 accuracy of 83.15% and a Top-3 accuracy of 95.75%.

These results highlight the effectiveness of VideoCLIP and Multi-frameCLIP in leveraging temporal information from video data for improved performance. It is important to note that we conduct comprehensive testing across various hyperparameter settings and select the parameters that deliver the highest performance for our proposed models. We refer to this setting as the ‘‘optimal hyperparameter setting’’. A detailed analysis of these results and a discussion of the optimal hyperparameter setting are presented in the following sections.

1) Zero-shotCLIP results

For the zero-shot experiments, we test the Zero-shotCLIP model on the distracted driving dataset without any prior training. The model encounters previously unseen frames extracted from distracted driving datasets. The RGB input images are resized to a resolution of 224x224x3. During the zero-shot evaluation, the framework extracts visual and textual features from the input images and corresponding textual prompts. Subsequently, the cosine similarity between these visual and textual features is computed, resulting in a ranked list of the most probable classes based on their similarity scores. The

zero-shot transfer results are presented in Table III for different CLIP backbones. It can be seen that the ViT-L/14@336px vision transformer-based Zero-shotCLIP outperforms other variants in terms of Top-1 accuracy. It should be noted that the ViT-L/14@336px backbone processes input images at a higher RGB resolution (336x336x3). A key observation from this table is that ViT-L/14@336px based Zero-shotCLIP reached up to 86.33% Top-3 accuracy in the SAM-DD dataset without requiring dataset-specific training.

TABLE III
ZERO-SHOT TRANSFER RESULTS

CLIP backbones	SynDD1		DMD		SAM-DD	
	Top-1	Top-3	Top-1	Top-3	Top-1	Top-3
ViT-L/14	53.50	74.50	47.97	79.56	62.51	84.52
ViT-L/14@336px	54.00	65.00	48.12	77.16	66.52	86.33
ViT-B/16	47.50	64.50	31.29	54.95	18.67	79.18
ViT-B/32	38.00	45.50	28.39	47.76	10.48	40.09

2) Single-frameCLIP results

We demonstrate the performance of the Single-frameCLIP model with optimal hyperparameter setting on the four datasets in Table IV. Single-frameCLIP results showcase the advantage of task-based fine-tuning over Zero-shotCLIP. For the SAM-DD dataset, the Single-frameCLIP model with the ViT-L/14 backbone achieved a Top-1 accuracy of 89.14% with the side-view frames. On the SynDD1 dataset, the same model reached a Top-1 accuracy of 57.35%. The results further confirm the robustness and effectiveness of the ViT-L/14-based backbones in the Single-frameCLIP model for distracted driving recognition tasks. It should be noted that the ‘leaving a set of driver out’ and the k -fold cross-validation method played a vital role in determining the optimal hyperparameter setting.

TABLE IV
SINGLE-FRAMECLIP RESULTS WITH OPTIMAL HYPERPARAMETERS

Single-frameCLIP backbone	Dataset	Camera view	Top-1 accuracy	Leaving a set of driver out
ViT-L/14	StateFarm	Side-view	83.15	✓
ViT-L/14	SynDD1	Dashboard	57.35	✓
ViT-L/14@336px	DMD	Side-view	82.65	✓
ViT-L/14	SAM-DD	Side-view	89.14	✓

3) Multi-frameCLIP results

The Multi-frameCLIP framework involves employing majority voting over a set of consecutive frames to determine the final prediction of an action in a video clip. We investigate various sampling rates of 0.5, 1, 2, 5, and 20 frames per second, subject-level cross-validation along with different camera views and CLIP backbones. The result with the optimal setting is presented in Table V. The best performance is achieved with the ViT-L/14@336px backbone on the DMD dataset for the side-view video clip sampled at 1 frame per second. This optimal setting provided a Top-1 accuracy of 93.39%. We have observed that the model achieves peak performance at a sampling rate of 1 FPS. Any increase in the sampling rate resulted in a decline in accuracy (as shown in Table XIII) since the inclusion of similar-looking frames acts as a form of noisy

signal in the majority voting pool. On the other hand, reducing the sampling rate below 1 compromised the performance since critical temporal information that is essential for final action prediction gets overlooked. Therefore, we can conclude that 1 FPS is the optimal sampling rate for the Multi-frameCLIP model to adequately capture relevant temporal information. The main advantage of this model is that it processes several frames simultaneously, exploiting the temporal information between two consecutive frames. This approach, combined with the high-level semantic understanding of the CLIP model, resulted in an improved performance. The optimal hyperparameters were determined through a series of experiments to optimize the model’s overall performance.

TABLE V
MULTI-FRAMECLIP RESULTS WITH OPTIMAL HYPERPARAMETERS

Multi-frameCLIP backbone	Dataset	FPS	Camera view	Top-1 accuracy	Leaving a set of driver out
ViT-L/14	SynDD1	1	Dashboard	70.36	✓
ViT-L/14@336px	DMD	1	Side-view	93.39	✓
ViT-L/14	SAM-DD	1	Side-view	89.14	✓

4) VideoCLIP results

TABLE VI
VIDEOCLIP RESULTS WITH OPTIMAL HYPERPARAMETERS

VideoCLIP backbone	Dataset	FPS	Camera view	Top-1 accuracy	Leaving a set of driver out
ViT-L/14	SynDD1	20	Dashboard	81.85	✓
ViT-L/14@336px	DMD	1	Side-view	98.44	✓
ViT-L/14	SAM-DD	1	Side-view	97.86	✓

Similar to Multi-frameCLIP, we conduct a series of tests to obtain the optimal hyperparameter setting for the VideoCLIP model and report the results in Table VI. The best performance of 97.86% Top-1 accuracy is achieved on the SAM-DD dataset with the ViT-L/14 backbone and with a sampling rate of 1 frame per second. The performance achieved by the VideoCLIP model validates its efficacy in understanding distracted actions from driving video footage. We have observed that the sampling rate has a significant effect on the final accuracy. Moreover, in contrast to Multi-frameCLIP, VideoCLIP uses a sliding window of 30 frames and employs a majority voting scheme on the outputs of these small video clips. It is important to note that on the SynDD1 dataset, the VideoCLIP achieved the best performance at 20 FPS sampling rate. If the sampling rate is too small, e.g., 1 FPS, there will be one frame sampled from every second of an activity. Since VideoCLIP uses 30 frames to build a video clip, this clip will span 30 seconds which can be longer than the average action duration (from Fig. 5 the average action duration for SynDD1 dataset is ~ 18.7 sec) and confuse the network. For example, an action video lasting 20 seconds should contain 20 frames at 1FPS; however, in these 20 frames, only 10 frames contain valid information about that action. Now, if we sample 30 frames from those 20 frames to make up a window as the input to the VideoCLIP network, most frames in that window are noise. In addition, the sliding window approach in VideoCLIP provides a more holistic representation of the video data, which leads

to improved prediction accuracy. In the following sections, we will delve into the performance of our models under real-world variabilities and scrutinize the model’s efficacy across diverse scenarios.

B. Performance Comparison with Other Works

In this section, we present a performance comparison of our proposed CLIP-based frameworks (both frame-based and video-based) with traditional distracted driving recognition models.

1) Single-frameCLIP vs. Traditional Models

In this section, we compare the performance of the Single-frameCLIP model with traditional distracted driving backbones on frame-based datasets. We provided two distinct tables to highlight how the accuracy scores change across different test driver sets and model backbones on the StateFarm and SynDD1 datasets. The Top-1 accuracy scores from our runs are presented in Tables VII, VIII and Fig. 6. It should be noted that, across all model comparisons in our experiments, we maintain consistency by using the same experimental settings along with the same action classes. Table VII shows the detailed breakdown of our ‘leave a set of drivers out’ approach that we used for testing on the StateFarm dataset. The first column entries represent the drivers included in the testing split. This data split involved leaving three drivers out for testing. For instance, ‘p002p014p012’ signifies that drivers with driverIDs ‘p002’, ‘p014’, and ‘p012’ were considered for the test set in the first fold. The remaining drivers were used for the training set. We follow this procedure eight times, each time keeping different groups of drivers separate for testing. We conduct 8-fold driver-level cross-validation on the StateFarm dataset. The other columns display the Top-1 accuracy of each model for different test splits. The last row provides an average Top-1 accuracy for each model across all folds. Amongst all the models, the Single-frameCLIP model with ViT-L/14 architecture emerged as the best performing, achieving an average Top-1 accuracy of 83.15%. Fig. 6 visually represents these results. The bars illustrate the average Top-1 accuracy of the models, while the vertical lines on the top indicate the variance in Top-1 accuracies across all eight folds.

TABLE VII
SINGLE-FRAMECLIP VS. TRADITIONAL MODELS:
TOP-1 ACCURACY ON STATEFARM DATASET

Test DriverID	ResNet18	MobileNet-v2	AlexNet	ViT-L/14
p002p014p012	72.81	74.09	68.23	75.66
p015p016p021	81.35	82.16	75.33	88.12
p024p022p026	87.11	86.16	81.67	89.03
p041p039p035	87.17	85.60	87.12	90.27
p042p045p047	84.00	81.91	81.72	89.03
p051p049p050	88.72	81.48	70.38	78.13
p061p056p052	86.17	82.50	75.16	72.39
p066p072p064	74.14	66.45	59.14	71.46
Avg. Top-1	82.68	80.04	74.84	83.15

The results obtained with the eight distracted driving classes in the SynDD1 dataset are presented in Table VIII. Similar to the experiments on the StateFarm dataset, this experiment involved 7-fold driver-level cross-validation with ‘leaving two

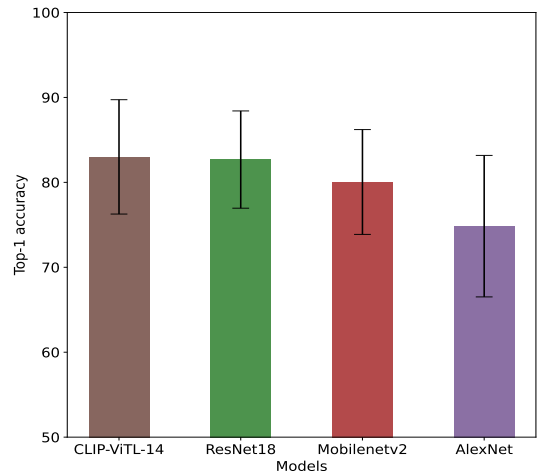


Fig. 6. The average Top-1 accuracy of Single-frameCLIP and other baselines on the StateFarm dataset. We perform 8-fold cross-validation and show the mean and variance of Top-1 accuracy values across all the folds along the Y-axis.

TABLE VIII
SINGLE-FRAMECLIP VS. TRADITIONAL MODELS
TOP-1 ACCURACY ON SYNDD1 DATASET

Models	Backbones	Average Top-1 accuracy	Leaving a set of driver out
Single-frameCLIP	ViT-L/14	57.347	✓
	ViT-B/16	48.940	✓
	RN101	48.521	✓
	ViT-B/32	35.382	✓
Traditional Models	ResNet18	42.621	✓
	MobileNet-v2	36.102	✓
	AlexNet	13.712	✓

drivers out’ for testing in each fold. The third column in Table VIII represents the average Top-1 accuracy across all the 7-folds. The results reveal that the ViT-L/14 model outperformed others, achieving a Top-1 accuracy of 57.347% (average accuracy across 7-folds). The remaining models followed with lower accuracies, with ViT-B/16 achieving 48.940% and RN101 at 48.521%. In conclusion, the Single-frameCLIP model with the ViT-L/14 architecture demonstrated superior performance in terms of Top-1 accuracy both in the StateFarm and SynDD1 datasets.

2) Dataset size vs. Performance

In an effort to analyze the performance of the Single-frame CLIP model with smaller amounts of training data, a series of experiments were conducted utilizing a progressively reduced training dataset. In this experiment, we train the traditional models and our proposed CLIP-based frameworks in a similar experimental setting on the StateFarm dataset. We separate 3 drivers (driverID p012, p014, p021) for testing and progressively removed four drivers from the training set to create a smaller training set, which is 80%, 60%, 40%, and 20% of the original training set. For this process, instead of randomly removing frames, we reduce the training data based on the driverID since, in real-world scenarios, the model will be expected to generalize its learning to new, unseen drivers. The percentage of training data, the number

of drivers present in those splits, and the number of samples are shown in Table IX. For this experiment on the StateFarm dataset, we employ an 8-fold cross-validation scheme where we excluded three drivers (driverID p012, p014, p021) from every fold and used them as test subjects. We picked the ViT/L-14 backbone for the Single-frameCLIP. All the models used the same training samples and were finally tested on the same test set. The outcomes are presented in Fig. 7. The results suggest that reducing the size of the training set does not necessarily compromise the Single-frameCLIP model’s performance. Unlike the other models assessed, which displayed a decrease in accuracy, the Single-frameCLIP model maintained its performance levels consistently even when the quantity of training data was reduced to 20% of the original amount.

TABLE IX
TRAINING DATASIZE FOR REDUCED TRAINING SET

Percentage of training data	No. of drivers in training	No. of samples in training	Test set driver IDs
80%	18	16163	p012p014p021
60%	14	12900	p012p014p021
40%	9	8949	p012p014p021
20%	5	5649	p012p014p021

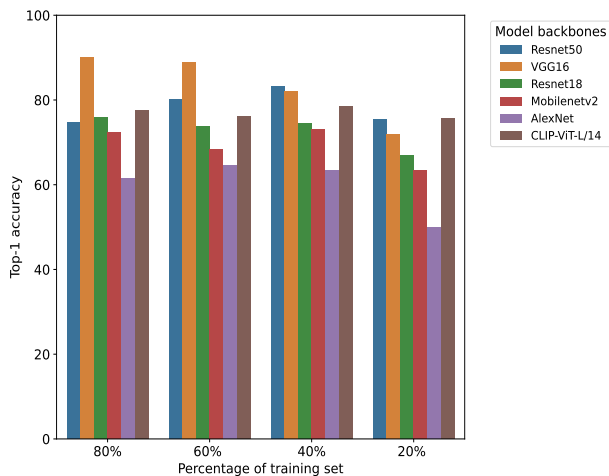


Fig. 7. Performance comparison of the Single-frameCLIP model and traditional models trained on varying proportions of the StateFarm dataset. Training sets of 80%, 60%, 40%, and 20% were created by progressively removing drivers based on their driverID. The figure reports the models’ average accuracies obtained through an 8-fold cross-validation scheme based on driverID.

3) Multi-frameCLIP vs. Traditional Models

We provide an extensive performance comparison of Multi-frameCLIP with traditional models on three different datasets in Table XIII. To ensure consistency and reliability in our experiments, we run the listed models at a 1FPS sampling rate with the same 7-fold cross-validation and ‘leaving a set of driver out’ settings across all the datasets. The Multi-frameCLIP model shows superior performance compared to the other baselines, achieving a Top-1 accuracy of 93.39% on DMD, 89.14% on SAM-DD, and 70.36% on the SynDD1 dataset. These results are significantly higher than those of

TABLE X
MULTI-FRAMECLIP VS. TRADITIONAL MODELS
(AT SAMPLING RATE 1FPS)

Video Datasets	Models	Top-1 Acc.(%)	Modality	Leaving a set of driver out
DMD	AlexNet	45.86	RGB	✓
	VGG16	56.15	RGB	✓
	MobileNet-v2	85.77	RGB	✓
	ResNet18	85.95	RGB	✓
	Multi-frameCLIP	93.39	RGB	✓
SAM-DD	VGG16	86.93	RGB	✓
	AlexNet	88.50	RGB	✓
	MobileNet-v2	92.95	RGB	✓
	Multi-frameCLIP	89.14	RGB	✓
SynDD1	AlexNet	12.56	RGB	✓
	VGG16	12.56	RGB	✓
	MobileNet-v2	33.65	RGB	✓
	ResNet50	43.49	RGB	✓
	ResNet18	47.55	RGB	✓
	Multi-frameCLIP	70.36	RGB	✓

models such as AlexNet, VGG16, MobileNet-v2, and ResNet variants when tested under the same conditions. In addition, it showcases the Multi-frameCLIP model’s efficacy in capturing driver behavior in different scenes, making it a suitable benchmark for distracted driving detection applications. However, it is important to note that accuracy fluctuates with changes in hyperparameters such as model type, sampling rate, camera view, and so on (discussed in the following sections), indicating that these are significant factors to consider to get an optimized performance.

4) VideoCLIP vs. Traditional Models

We showcase a comparative analysis of the VideoCLIP against the traditional baselines in Table XI. It shows that VideoCLIP gets significant performance gain and outperforms its counterparts across three different datasets. On the DMD dataset, VideoCLIP outperforms all other models, including advanced configurations like MobileNet-v2 (MLP), 3D CNN variants and modalities, achieving a Top-1 accuracy of 98.44%. Similarly, in the SAM-DD dataset, VideoCLIP tops the chart with 97.86% accuracy, surpassing other SOTA models such as Swin Transformers and ViTs. Furthermore, on the SynDD1 dataset, VideoCLIP maintains its lead with an 81.85% accuracy at a 20FPS rate, which is substantially higher than the average Top-1 accuracy of the competing model [69]. These results highlight the efficacy of the VideoCLIP model in harnessing RGB modality and underscore its robustness across different datasets within the ‘leave a set of driver out’ setting.

C. Hyperparameters and Ablation Studies

In this section, we discuss how various real-world parameter settings, such as the sampling rate, camera location and presence of different distracted driving classes can impact the performance of our proposed CLIP-based frameworks.

1) Sampling Rate

To see the effect of sampling rates on model performance, we test Multi-frameCLIP and VideoCLIP at various sampling rates on the SynDD1 dataset. Table XIII and Table XIV show the results. We maintain the same experimental settings and observe distinct trends across different sampling rates.

TABLE XI
VIDEOCLIP VS. TRADITIONAL MODELS
(WITH SAMPLING RATE 1FPS)

Video Datasets	Models	Top-1 Acc.(%)	Modality	Leaving a set of driver out
DMD	ShuffleNet-v2	84.80	RGB	x
	3D-ShuffleNet-v2	88.50	RGB	x
	MobileNet-v2	89.90	RGB	x
	MobileNet-v2	85.77	RGB	✓
	3D-MobileNet-v2	90.30	RGB	x
	MobileNet-v2(MLP)	91.60	RGB	x
	Inception-v3	91.80	RGB	x
	MobileNet-v2(MLP)	93.70	RGB+IR+D	x
	MobileNet-v2(MLP) [35]	93.90*	IR+D	x
	VideoCLIP	98.44	RGB	✓
SAM-DD	MobileNet-v3	94.78	RGB	✓
	ShuffleNet-v2	95.56	RGB	✓
	ResNet18	95.91	RGB	✓
	VGG16	96.86	RGB	✓
	ViT	97.09	RGB	✓
	Swin-T [4]	97.33*	RGB	✓
	VideoCLIP	97.86	RGB	✓
SynDDI	VideoMAE [69]	71.35**	RGB	✓
	VideoCLIP(1FPS)	74.64	RGB	✓
	VideoCLIP(20FPS)	81.85	RGB	✓

*best performing model proposed by the author

**average Top-1 accuracy for the same classes used in VideoCLIP

TABLE XII
SINGLE-FRAMECLIP: F1-SCORE ON DMD AND SAM-DD

Action class	F1-score DMD	F1-score SAM-DD
drinking water	0.96	0.98
hair and makeup	0.91	0.84
talking to phone	0.97	0.96
adjusting radio	0.86	-
reaching to backseat	0.68	0.91
reaching to side	0.58	-
driving safely	0.68	0.93
talking to passenger	0.87	-
texting on phone	0.92	0.84
yawning	0.76	-

The ViT-L/14-based Multi-frameCLIP achieves the peak Top-1 accuracy at a 1 FPS sampling rate with an accuracy of 70.36%. This was the highest accuracy achieved across all tested models and sampling rate settings for this experiment. In comparison, the AlexNet and VGG16 models got the lowest accuracy values. However, in Table XIV the VideoCLIP achieves the highest Top-1 accuracy at 20 FPS, with an accuracy of 81.85%. This contrast highlights the models’ sensitivity to sampling rate variations, suggesting that the optimal rate depends on the specific model and dataset characteristics. The changes from one frame to the next are more significant at a 1 FPS sampling rate, which helped the Multi-frameCLIP model make more accurate predictions. Therefore, 1 FPS is the optimal sampling rate for the Multi-frameCLIP model under the conditions of our study. On the other hand, as the average action duration for the SynDD1 dataset is ~18.7 sec, a 20FPS rate results in a better temporal resolution, allowing the VideoCLIP model to capture more subtle changes and movements. If the sampling rate is too small, then the video clip will span more than the average action duration and confuse the model prediction. Therefore, the impact of the sampling rate would depend on the average action duration

and the characteristics of the downstream tasks.

2) Class-level Analysis

We illustrate the class-level F1-scores of Single-frameCLIP on the DMD and SAM-DD datasets in Table XII. In this table, we analyze the ten classes of the datasets to understand the most challenging actions to classify. The average F1-scores on DMD and SAM-DD datasets are 0.819 and 0.847, respectively. In addition, we demonstrate the confusion matrix of Single-frameCLIP on fold02 of the DMD dataset as an example in Fig. 8. We have found that the DMD classes such as “reaching to backseat”, “reaching to side” and “driving safely” exhibited lower F1-scores (<0.70), indicating that these categories pose greater challenges for the framework to classify correctly. These action classes appeared to generate similar image features, leading to a higher rate of misclassification. Additionally, we noticed that only two SAM-DD classes “head dropping” and “touching hair” got F1-scores below 0.70 among the ten classes. To further illustrate this, Fig. 9 provides visual examples of instances where the Single-frameCLIP model incorrectly classified actions, comparing the model’s outputs against the ground truth.

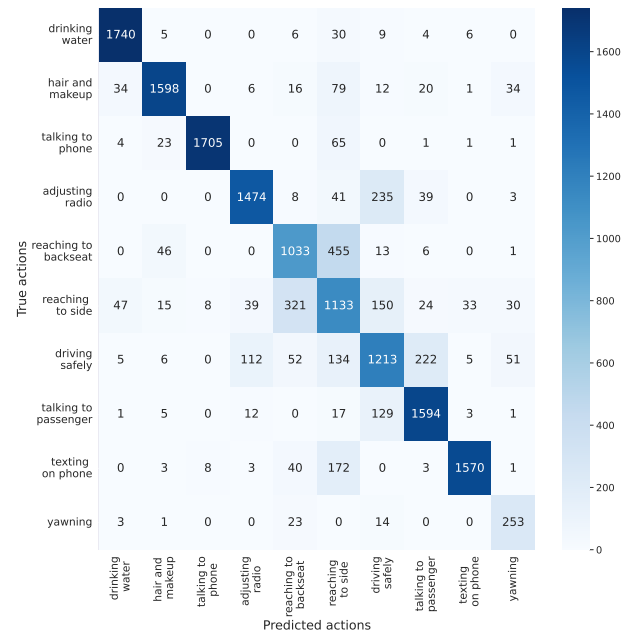


Fig. 8. Confusion matrix of Single-frameCLIP model on DMD dataset. It shows that the “reaching to backseat”, “reaching to side” and “driving safely” classes were the most challenging for the Single-frameCLIP model. Also, the dataset has limited “yawning” samples compared to the other classes. Additionally, we noticed that only two SAM-DD classes “head dropping” and “touching hair” got F1-scores below 0.70 among the ten classes.

3) Merging and Removing Classes

To fully understand the impact of the challenging classes on overall model performance, we pursue two additional experiments: merging and removing classes. Our initial focus was to explore how the overall model performance is influenced by either merging or removing classes that are more challenging to predict accurately. From our previous analysis, we noticed that the Single-frameCLIP model has difficulty in accurately predicting the “singing”, “eating” and “yawning” classes on the SynDD1 dataset compared to other classes.

TABLE XIII
MULTI-FRAMECLIP AT DIFFERENT SAMPLING RATES ON SYNDD1 DATASET (WITH LEAVING A SET OF DRIVER OUT)

Sampling Rate	ViT-L/14	ViT-B/16	RN101	ViT-B/32	ResNet18	ResNet50	Modilenetv2	AlexNet	VGG16
0.5FPS	56.67%	52.98%	48.57%	39.52%	43.51%	39.52%	41.31%	12.62%	12.62%
1FPS	70.36%	60.01%	55.60%	41.65%	47.55%	43.49%	33.65%	12.56%	12.56%
2FPS	59.46%	53.04%	50.36%	37.68%	40.59%	38.75%	34.11%	12.62%	12.62%
5FPS	62.08%	59.34%	49.34%	36.96%	43.21%	39.70%	48.75%	12.62%	12.62%
20FPS	61.25%	61.13%	49.35%	36.96%	46.79%	40.71%	45.12%	12.62%	12.62%

TABLE XIV
VIDEOCLIP AT DIFFERENT SAMPLING RATES ON SYNDD1 DATASET (WITH LEAVING A SET OF DRIVER OUT)

Sampling Rate	Fold0	Fold1	Fold2	Fold3	Fold4	Fold5	Fold6	Mean
1FPS	93.75%	87.50%	87.50%	75.00%	60.00%	50.00%	68.75%	74.64%
2FPS	81.25%	87.50%	87.50%	87.50%	66.67%	68.75%	75.00%	79.17%
5FPS	87.50%	81.25%	93.75%	75.00%	66.67%	56.25%	68.75%	75.60%
20FPS	87.50%	93.75%	87.50%	93.75%	66.67%	68.75%	75.00%	81.85%

TABLE XV
SINGLE-FRAME CLIP: REMOVING VS. MERGING CLASSES RESULTS ON SYNDD1 DATASET

Experiment type	No.of class	No.of camera-view	adjusting hair	drinking water	picking something	reaching behind	talking phone	sing+eat +yawn	Mean F1	Mean accuracy
Removing	5	3	0.64	0.71	0.84	0.82	0.80	-	0.763	75.62%
Merging	6	3	0.51	0.50	0.82	0.75	0.88	0.73	0.698	69.41%
Removing with dashboard-view	5	1	0.77	0.87	0.89	0.94	0.89	-	0.873	87.08%

Table XV reflects our findings, which are categorized into three different experimental settings. The first row shows the outcome following the removal of the three challenging classes with three camera views. This modification resulted in an average F1 score of 0.763 and a mean accuracy of 75.62%. The second row illustrates the outcome of merging the three challenging classes with three camera views. This scenario led to a mean F1 score of 0.698 and an average accuracy of 69.41%. The third row provides the results obtained from an experiment in which the three challenging classes were removed and only the dashboard camera view was considered. This experimental setup led to an average F1 score of 0.873 and a mean accuracy of 87.08%. In conclusion, the optimization of the camera views, combined with the adjustment of the challenging classes, resulted in a significant improvement in the model’s performance.

4) Effect of Camera Views

In this section, we investigate the effect of camera position on our framework’s performance. In Table XVI, we present the Top-1 accuracy for Single-frameCLIP and Multi-frameCLIP on ten distracted classes for the SAM-DD dataset, considering two distinct camera views. The outcomes suggest that the side

TABLE XVI
EFFECT OF CAMERA-VIEW ON SAM-DD DATASET

Models (ours)	Camera view	Top-1 accuracy	Leaving a set of driver out
Single-frameCLIP	Dashboard	88.919	✓
	Side-view	89.142	✓
Multi-frameCLIP	Dashboard	88.908	✓
	Side-view	89.142	✓

view yields superior results when compared to the dashboard camera view. These results underscore the significance of the camera’s perspective in detecting driver distractions. The side camera view appears to provide the most effective angle for the SAM-DD dataset, capturing the driver’s movements and body maneuvers.

D. Computational Complexity

TABLE XVII
VIDEOCLIP COMPUTATION EFFICIENCY (BATCH SIZE=1)

FLOPs (G)	#Params. (M)	Forw./backw. pass size(MB)	Params size (MB)	Estimated Total size(MB)
3.54	9.67	964.26	38.68	1021

In Table XVII, we present the details of the computational efficacy of the proposed VideoCLIP model. In terms of driver distraction recognition tasks, we compared the floating point operations (FLOPs) and the number of parameters (#Params.) of VideoCLIP with its counterparts. VideoCLIP demonstrates superior FLOPs efficiency and a relatively smaller parameter count (<10M). For example, in the SAM-DD dataset [4] setting, Swin-T gets 4.5G FLOPs and 28.3M trainable parameters. In [69] setting, VideoMAE operates at 57G FLOPs with 22M parameters, ResNet50 [42] uses 3.8 GFLOPs with 25.6M parameters for an input size of 224x224x3. Therefore, the computational performance of the VideoCLIP model coupled with a Top-1 accuracy of 81.85% makes it a resource-effective model in the driver distraction recognition task context. This efficiency is particularly valuable in real-time Intelligent Transportation applications like driver distraction recognition,

where quick and accurate video processing is essential for safety and effectiveness. Moreover, the small parameter count also implies potentially lower memory requirements and faster training times, further enhancing its applicability in practical scenarios.

E. Anecdotal Observation

In this section, we discuss the cases where our proposed frameworks struggle to perform well and investigate the possible reasons.

1) Failure cases

We demonstrate some miss-classified frames from the Single-frameCLIP model on DMD and SynDD1 dataset in Fig. 9 and the class-level confusion matrix of DMD classes in Fig 8. Analyzing the confusion matrix and the miss-classified frames, it is evident that the most challenging classes for the model occur where there is considerable feature overlap between classes that exhibit lower F1-scores. The middle column of Fig 9 shows the overlapping cues between two actions characterized by specific hand movements or facial expressions.



Fig. 9. Some example frames that were misclassified by the Single-frameCLIP on DMD (top row) and SynDD1 (bottom row). These examples show evidence of how Single-frameCLIP fails to capture the temporal information only by looking at a single frame at a time.

For example, the first-row middle frame driver’s left-hand position close to the steering wheel resembles the starting motion to the side, which confused the model to incorrectly predict the “reaching side” class. Therefore, the Single-frameCLIP model struggles to distinguish actions where the visual movements are subtle and there is a slight temporal context. Most of the time, it is quite complicated to decipher these activities only by looking at a single frame. To address this issue, the Multi-frameCLIP and VideoCLIP frameworks were developed, where a sequence of consecutive frames is assessed for a more accurate prediction score. Moreover, these models leverage the temporal information across multiple frames and capture subtle changes in hand movements and facial gestures. This consideration contributed to a significant performance enhancement relative to the Single-frameCLIP model.

2) Frame-by-frame Analysis on SynDD1 Video Clips

Fig. 10 presents the frame-by-frame analysis of video input for driverID 25470 from the SynDD1 dataset using the Multi-frameCLIP and VideoCLIP models. The depicted plot

conveys the dynamic probabilities of predictions produced by the Multi-frameCLIP and VideoCLIP models over the entire span of action. The vertical axis shows the moving average of the computed probabilities in relation to the individual frame numbers, represented by the horizontal axis. We observe distinct fluctuations between high and low probability scores, aligning with frames where the model either successfully or unsuccessfully classified the given action. Our analysis focused on two distinct actions - adjusting hair and singing, at a sampling rate of 20 FPS. The representation of lower and higher probability scores from both models is clearly distinguished in this visualization. An important observation is the superiority of VideoCLIP’s prediction score over the entire course of action compared to that of the Multi-frameCLIP model. Additionally, we notice that VideoCLIP demonstrates a stable and consistent performance, capturing low-probability frames and maintaining a consistent score throughout the video. In contrast, the Multi-frameCLIP model appears to struggle at certain frames. Therefore, we conclude that VideoCLIP has the capability to efficiently capture temporal information from videos, significantly improving prediction accuracy while maintaining consistency. Moreover, the plot illustrates the superiority of both Multi-frameCLIP and VideoCLIP in extracting the temporal correlations among frames, thus providing insights into continuous actions that are challenging to get from isolated frames, as in the Single-frameCLIP scenario.

F. Limitations and Future directions

Our algorithm shows promising results within its current setup, yet there is potential to further its adaptability and performance in varied real-world driving conditions across different unusual distraction categories. The variety of distractions that drivers encounter is vast and often unpredictable. Therefore, we need a sophisticated monitoring system to recognize the natural interactions between humans and vehicles and encourage safe driving practices. This system must be equipped to accurately identify the driver’s current state and assess the reliability of its predictions. Our current models were tested under controlled and available distracted settings from public datasets. The performance and efficacy in real-world applications, considering diverse hardware and environmental conditions, were not fully explored. To enhance the robustness and applicability of our algorithm, future work could involve training with additional data that cover a wider range of driving conditions - multiple distracted behaviors occurring simultaneously or alternately, unexpected or out-of-distribution behavior categories, occlusion events and so on. This would help in validating the algorithm’s effectiveness across various scenarios. Optimizing the algorithm for efficient performance across a range of hardware platforms, including low-power devices or with limited compute resources, could be a significant area of focus. This would make the system more viable for real-time applications in vehicles. Additionally, future research should also consider the ethical implications and privacy concerns associated with driver monitoring, ensuring compliance with relevant regulations and societal norms. Also,

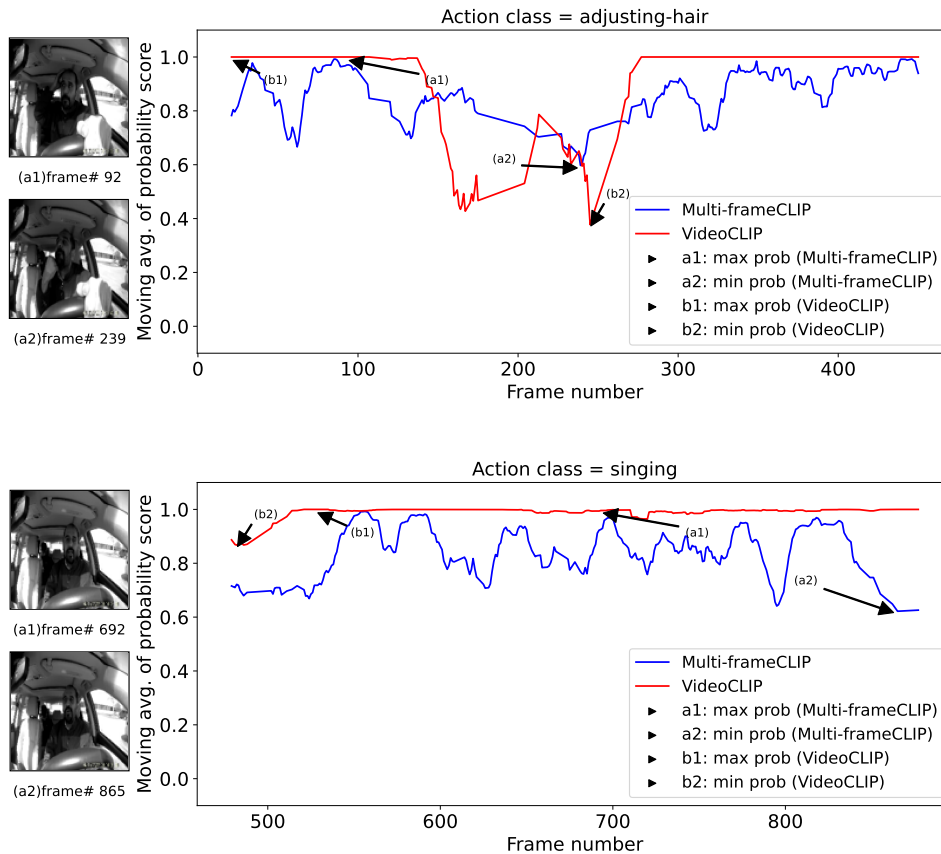


Fig. 10. This plot shows the predicted probability score vs. frame number. We analyze the Multi-frameCLIP and VideoCLIP model’s prediction probability scores for the entire action. We notice distinct changes in frames for high and low probability scores. This figure demonstrates that VideoCLIP outperforms Multi-frameCLIP’s prediction scores, offering a better approach to capturing temporal features. Therefore, VideoCLIP performs better in classifying actions on video data

we plan to address the misclassification issues (discussed in V-E1) and enhance the reliability of the model predictions by implementing reliable uncertainty estimates [70]. This would be particularly beneficial in complex or ambiguous scenarios where driver behavior is not distinctly classifiable, thus allowing for a more nuanced understanding and interpretation of the model’s confidence measures. We believe that this addition will enhance the safety and reliability of the automated driver assistance systems by providing a more comprehensive and trustworthy analysis of driver behavior.

VI. CONCLUSION

In this paper, we have introduced a vision-language modeling framework aimed at categorizing distracted driving behaviors from naturalistic driving data. The performance of various CLIP-based frameworks has been evaluated on four common distracted driving datasets. Compared to the Zero-shotCLIP model, the Single-frameCLIP model benefited from task-based fine-tuning with significant improvement in accuracy while failing to capture the temporal dynamics of a video. Further experiments have shown that Multi-frameCLIP and VideoCLIP can leverage temporal information from video data, which allows for a better understanding of actions, events and sequences within a video. VideoCLIP and Multi-frameCLIP

frameworks have outperformed Single-frameCLIP by a significant margin. Overall, our proposed frameworks exhibit state-of-the-art performance at distracted action classification and outperform traditional and most widely used models. This study has also evaluated the efficacy of different CLIP-model backbones, highlighting that a variety of factors, including variable training dataset size, sampling rates, and camera angles, can influence their performance. These observations can contribute to the development of more robust driver assistance systems to understand driver distractions. This study emphasizes the real-world applicability and generalizability of these models while also pointing out areas for improvement, such as handling unexpected and out-of-distribution driving behavior categories and fine-tuning hyperparameters. Several future works could extend and refine our current CLIP-based driver distraction recognition model. First, exploring the optimization of prompts for Vision-Language foundation models may enable the framework to extract more nuanced visual-textual relationships, leading to an improved classification. Second, the fusion of different camera views can be investigated to deal with occlusion, provide a more comprehensive picture of driver behavior and make accurate decision-making.

Moreover, the generalizability of our model across various scenarios and datasets presents another intriguing prospect. For instance, assessing whether the model could be fine-tuned

on one dataset and subsequently deployed on another could further illustrate its versatility and effectiveness. In addition, we recognize the importance of empirical validation and testing our system under more challenging, unexpected, and out-of-distribution driving behavior categories. To this end, we are actively planning an extension of our current work. This next phase will include a series of experiments specifically designed to evaluate our framework's response to real-world out-of-distribution actions. We also aim to extend the model's testing to include a broader spectrum of actions, particularly focusing on those that are rare or challenging to classify. These tests are intended to validate our framework's robustness and enhance its adaptive capabilities further. Finally, systematic evaluations under diverse environmental conditions, such as varying lighting conditions and data quality, could offer valuable insights into the model's robustness and ability to function optimally under real-world driving circumstances.

REFERENCES

- [1] T. A. Dingus, F. Guo, S. Lee, J. F. Antin, M. Perez, M. Buchanan-King, and J. Hankey, "Driver crash risk factors and prevalence evaluation using naturalistic driving data," *Proceedings of the National Academy of Sciences*, vol. 113, no. 10, pp. 2636–2641, 2016.
- [2] N. Moslemi, R. Azmi, and M. Soryani, "Driver distraction recognition using 3d convolutional neural networks," in *2019 4th International Conference on Pattern Recognition and Image Analysis (IPRIA)*, 2019, pp. 145–151.
- [3] B. Li, J. Chen, Z. Huang, H. Wang, J. Lv, J. Xi, J. Zhang, and Z. Wu, "A new unsupervised deep learning algorithm for fine-grained detection of driver distraction," *IEEE Transactions on Intelligent Transportation Systems*, vol. 23, no. 10, pp. 19 272–19 284, 2022.
- [4] H. Yang, H. Liu, Z. Hu, A.-T. Nguyen, T.-M. Guerra, and C. Lv, "Quantitative identification of driver distraction: A weakly supervised contrastive learning approach," *IEEE Transactions on Intelligent Transportation Systems*, pp. 1–12, 2023.
- [5] S. Xie, C. Sun, J. Huang, Z. Tu, and K. Murphy, "Rethinking spatiotemporal feature learning: Speed-accuracy trade-offs in video classification," in *Proceedings of the European Conference on Computer Vision (ECCV)*, September 2018.
- [6] A. Ramesh, M. Pavlov, G. Goh, S. Gray, C. Voss, A. Radford, M. Chen, and I. Sutskever, "Zero-shot text-to-image generation," in *Proceedings of the 38th International Conference on Machine Learning*, ser. Proceedings of Machine Learning Research, M. Meila and T. Zhang, Eds., vol. 139. PMLR, 18–24 Jul 2021, pp. 8821–8831.
- [7] A. Singh, R. Hu, V. Goswami, G. Couairon, W. Galuba, M. Rohrbach, and D. Kiela, "Flava: A foundational language and vision alignment model," in *Proceedings of the IEEE/CVF Conference on Computer Vision and Pattern Recognition*, 2022, pp. 15 638–15 650.
- [8] H. Bao, W. Wang, L. Dong, Q. Liu, O. K. Mohammed, K. Aggarwal, S. Som, S. Piao, and F. Wei, "VLMo: Unified vision-language pre-training with mixture-of-modality-experts," in *Advances in Neural Information Processing Systems*, A. H. Oh, A. Agarwal, D. Belgrave, and K. Cho, Eds., 2022. [Online]. Available: <https://openreview.net/forum?id=bydKs84JEyw>
- [9] J. Cho, J. Lei, H. Tan, and M. Bansal, "Unifying vision-and-language tasks via text generation," in *Proceedings of the 38th International Conference on Machine Learning*, ser. Proceedings of Machine Learning Research, M. Meila and T. Zhang, Eds., vol. 139. PMLR, 18–24 Jul 2021, pp. 1931–1942.
- [10] A. Radford, J. W. Kim, C. Hallacy, A. Ramesh, G. Goh, S. Agarwal, G. Sastry, A. Askell, P. Mishkin, J. Clark *et al.*, "Learning transferable visual models from natural language supervision," in *International conference on machine learning*. PMLR, 2021, pp. 8748–8763.
- [11] X. Zhou, R. Girdhar, A. Joulin, P. Krähenbühl, and I. Misra, "Detecting twenty-thousand classes using image-level supervision," in *Computer Vision—ECCV 2022: 17th European Conference, Tel Aviv, Israel, October 23–27, 2022, Proceedings, Part IX*. Springer, 2022, pp. 350–368.
- [12] M. Wang, J. Xing, and Y. Liu, "Actionclip: A new paradigm for video action recognition," *arXiv preprint arXiv:2109.08472*, 2021.
- [13] B. Feuer, A. Joshi, M. Cho, K. Jani, S. Chiranjeevi, Z. K. Deng, A. Balu, A. K. Singh, S. Sarkar, N. Merchant, A. Singh, B. Ganapathysubramanian, and C. Hegde, "Zero-shot insect detection via weak language supervision," in *2nd AAAI Workshop on AI for Agriculture and Food Systems*, 2023. [Online]. Available: <https://openreview.net/forum?id=VPDKe672pv>
- [14] H. Fang, P. Xiong, L. Xu, and W. Luo, "Transferring image-clip to video-text retrieval via temporal relations," *IEEE Transactions on Multimedia*, vol. 25, pp. 7772–7785, 2023.
- [15] M. Patrick, P.-Y. Huang, Y. Asano, F. Metzke, A. G. Hauptmann, J. F. Henriques, and A. Vedaldi, "Support-set bottlenecks for video-text representation learning," in *International Conference on Learning Representations*, 2021. [Online]. Available: <https://openreview.net/forum?id=EqoXe2zmhrh>
- [16] S. Ging, M. Zolfaghari, H. Pirsiavash, and T. Brox, "Coot: Cooperative hierarchical transformer for video-text representation learning," in *Advances in Neural Information Processing Systems*, H. Larochelle, M. Ranzato, R. Hadsell, M. Balcan, and H. Lin, Eds., vol. 33. Curran Associates, Inc., 2020, pp. 22 605–22 618. [Online]. Available: https://proceedings.neurips.cc/paper_files/paper/2020/file/ff0abbc0227c9124a804b084d161a2d-Paper.pdf
- [17] A. Sanghi, H. Chu, J. G. Lambourne, Y. Wang, C. Cheng, M. Fumero, and K. Malekshan, "Clip-forge: Towards zero-shot text-to-shape generation," in *2022 IEEE/CVF Conference on Computer Vision and Pattern Recognition (CVPR)*. Los Alamitos, CA, USA: IEEE Computer Society, jun 2022, pp. 18 582–18 592.
- [18] A. Jain, B. Mildenhall, J. T. Barron, P. Abbeel, and B. Poole, "Zero-shot text-guided object generation with dream fields," *CVPR*, 2022.
- [19] H. Xu, G. Ghosh, P.-Y. Huang, D. Okhonko, A. Aghajanyan, F. Metzke, L. Zettlemoyer, and C. Feichtenhofer, "VideoCLIP: Contrastive pre-training for zero-shot video-text understanding," in *Proceedings of the 2021 Conference on Empirical Methods in Natural Language Processing (EMNLP)*. Online: Association for Computational Linguistics, Nov. 2021.
- [20] H. Fang, P. Xiong, L. Xu, and Y. Chen, "Clip2video: Mastering video-text retrieval via image clip," *arXiv preprint arXiv:2106.11097*, 2021.
- [21] E. Ohn-Bar and M. M. Trivedi, "Looking at humans in the age of self-driving and highly automated vehicles," *IEEE Transactions on Intelligent Vehicles*, vol. 1, no. 1, pp. 90–104, 2016.
- [22] P. Li, M. Lu, Z. Zhang, D. Shan, and Y. Yang, "A novel spatial-temporal graph for skeleton-based driver action recognition," in *2019 IEEE Intelligent Transportation Systems Conference (ITSC)*, 2019, pp. 3243–3248.
- [23] M. Martin, J. Popp, M. Anneken, M. Voit, and R. Stiefelhagen, "Body pose and context information for driver secondary task detection," in *2018 IEEE Intelligent Vehicles Symposium (IV)*, 2018, pp. 2015–2021.
- [24] N. Das, E. Ohn-Bar, and M. M. Trivedi, "On performance evaluation of driver hand detection algorithms: Challenges, dataset, and metrics," in *2015 IEEE 18th International Conference on Intelligent Transportation Systems*, 2015, pp. 2953–2958.
- [25] L. Yang, K. Dong, A. J. Dmitruk, J. Brighton, and Y. Zhao, "A dual-cameras-based driver gaze mapping system with an application on non-driving activities monitoring," *IEEE Transactions on Intelligent Transportation Systems*, vol. 21, no. 10, pp. 4318–4327, 2020.
- [26] R. Oyini Mbouna, S. G. Kong, and M.-G. Chun, "Visual analysis of eye state and head pose for driver alertness monitoring," *IEEE Transactions on Intelligent Transportation Systems*, vol. 14, no. 3, pp. 1462–1469, 2013.
- [27] Q. Massoz, T. Langohr, C. François, and J. G. Verly, "The ulg multimodality drowsiness database (called drozy) and examples of use," in *2016 IEEE Winter Conference on Applications of Computer Vision (WACV)*, 2016, pp. 1–7.
- [28] X. Zuo, C. Zhang, F. Cong, J. Zhao, and T. Hämmäläinen, "Driver distraction detection using bidirectional long short-term network based on multiscale entropy of eeg," *IEEE Transactions on Intelligent Transportation Systems*, vol. 23, no. 10, pp. 19 309–19 322, 2022.
- [29] G. Li, W. Yan, S. Li, X. Qu, W. Chu, and D. Cao, "A temporal-spatial deep learning approach for driver distraction detection based on eeg signals," *IEEE Transactions on Automation Science and Engineering*, vol. 19, no. 4, pp. 2665–2677, 2022.
- [30] Y. Liang, M. L. Reyes, and J. D. Lee, "Real-time detection of driver cognitive distraction using support vector machines," *IEEE Transactions on Intelligent Transportation Systems*, vol. 8, no. 2, pp. 340–350, 2007.
- [31] A. Jain, H. S. Koppula, B. Raghavan, S. Soh, and A. Saxena, "Car that knows before you do: Anticipating maneuvers via learning temporal driving models," in *2015 IEEE International Conference on Computer Vision (ICCV)*. Los Alamitos, CA, USA: IEEE

- Computer Society, dec 2015, pp. 3182–3190. [Online]. Available: <https://doi.ieeecomputersociety.org/10.1109/ICCV.2015.364>
- [32] K. Ben Ahmed, B. Goel, P. Bharti, S. Chellappan, and M. Bouhorma, “Leveraging smartphone sensors to detect distracted driving activities,” *IEEE Transactions on Intelligent Transportation Systems*, vol. 20, no. 9, pp. 3303–3312, 2019.
- [33] R. Khosrowabadi, M. Heijnen, A. Wahab, and H. C. Quek, “The dynamic emotion recognition system based on functional connectivity of brain regions,” in *2010 IEEE Intelligent Vehicles Symposium*, 2010, pp. 377–381.
- [34] J. Wang, W. Chai, A. Venkatachalapathy, K. L. Tan, A. Haghghat, S. Velipasalar, Y. Adu-Gyamfi, and A. Sharma, “A survey on driver behavior analysis from in-vehicle cameras,” *IEEE Transactions on Intelligent Transportation Systems*, vol. 23, no. 8, pp. 10 186–10 209, 2022.
- [35] J. D. Ortega, N. Kose, P. Cañas, M.-A. Chao, A. Unnervik, M. Nieto, O. Otaegui, and L. Salgado, “Dmd: A large-scale multi-modal driver monitoring dataset for attention and alertness analysis,” in *Computer Vision – ECCV 2020 Workshops*, A. Bartoli and A. Fusiello, Eds. Springer International Publishing, 2020, pp. 387–405.
- [36] O. Kopuklu, J. Zheng, H. Xu, and G. Rigoll, “Driver anomaly detection: A dataset and contrastive learning approach,” in *Proceedings of the IEEE/CVF Winter Conference on Applications of Computer Vision*, 2021, pp. 91–100.
- [37] B. Qin, J. Qian, Y. Xin, B. Liu, and Y. Dong, “Distracted driver detection based on a cnn with decreasing filter size,” *IEEE Transactions on Intelligent Transportation Systems*, vol. 23, no. 7, pp. 6922–6933, 2022.
- [38] X. Shi, S. Shan, M. Kan, S. Wu, and X. Chen, “Real-time rotation-invariant face detection with progressive calibration networks,” in *Proceedings of the IEEE Conference on Computer Vision and Pattern Recognition*, 2018, pp. 2295–2303.
- [39] N. Kose, O. Kopuklu, A. Unnervik, and G. Rigoll, “Real-time driver state monitoring using a cnn based spatio-temporal approach,” in *2019 IEEE Intelligent Transportation Systems Conference (ITSC)*. IEEE, 2019, pp. 3236–3242.
- [40] P. Li, M. Lu, Z. Zhang, D. Shan, and Y. Yang, “A novel spatial-temporal graph for skeleton-based driver action recognition,” in *2019 IEEE Intelligent Transportation Systems Conference (ITSC)*. IEEE, 2019, pp. 3243–3248.
- [41] K. Simonyan and A. Zisserman, “Very deep convolutional networks for large-scale image recognition,” in *International Conference on Learning Representations*, 2015.
- [42] K. He, X. Zhang, S. Ren, and J. Sun, “Deep residual learning for image recognition,” in *2016 IEEE Conference on Computer Vision and Pattern Recognition (CVPR)*, 2016, pp. 770–778.
- [43] A. Krizhevsky, I. Sutskever, and G. E. Hinton, “Imagenet classification with deep convolutional neural networks,” in *Advances in Neural Information Processing Systems*, F. Pereira, C. Burges, L. Bottou, and K. Weinberger, Eds., vol. 25. Curran Associates, Inc., 2012. [Online]. Available: https://proceedings.neurips.cc/paper_files/paper/2012/file/c399862d3b9d6b76c8436e924a68c45b-Paper.pdf
- [44] C. Szegedy, V. Vanhoucke, S. Ioffe, J. Shlens, and Z. Wojna, “Rethinking the inception architecture for computer vision,” in *2016 IEEE Conference on Computer Vision and Pattern Recognition (CVPR)*, 2016, pp. 2818–2826.
- [45] M. Sandler, A. Howard, M. Zhu, A. Zhmoginov, and L.-C. Chen, “Mobilenetv2: Inverted residuals and linear bottlenecks,” in *Proceedings of the IEEE conference on computer vision and pattern recognition*, 2018, pp. 4510–4520.
- [46] N. Ma, X. Zhang, H.-T. Zheng, and J. Sun, “Shufflenet v2: Practical guidelines for efficient cnn architecture design,” in *Proceedings of the European conference on computer vision (ECCV)*, 2018, pp. 116–131.
- [47] M. Martin, A. Roitberg, M. Haurilet, M. Horne, S. Reiß, M. Voit, and R. Stiefelhagen, “Driveact: A multi-modal dataset for fine-grained driver behavior recognition in autonomous vehicles,” in *2019 IEEE/CVF International Conference on Computer Vision (ICCV)*, 2019, pp. 2801–2810.
- [48] J. Carreira and A. Zisserman, “Quo vadis, action recognition? a new model and the kinetics dataset,” in *proceedings of the IEEE Conference on Computer Vision and Pattern Recognition*, 2017, pp. 6299–6308.
- [49] K. Hara, H. Kataoka, and Y. Satoh, “Learning spatio-temporal features with 3d residual networks for action recognition,” in *Proceedings of the IEEE international conference on computer vision workshops*, 2017, pp. 3154–3160.
- [50] A. Diba, M. Fayyaz, V. Sharma, M. M. Arzani, R. Yousefzadeh, J. Gall, and L. Van Gool, “Spatio-temporal channel correlation networks for action classification,” in *Proceedings of the European Conference on Computer Vision (ECCV)*, 2018, pp. 284–299.
- [51] J. Stroud, D. Ross, C. Sun, J. Deng, and R. Sukthankar, “D3d: Distilled 3d networks for video action recognition,” in *Proceedings of the IEEE/CVF Winter Conference on Applications of Computer Vision*, 2020, pp. 625–634.
- [52] Y. Abouelnaga, H. M. Eraqi, and M. N. Moustafa, “Real-time distracted driver posture classification,” *arXiv preprint arXiv:1706.09498*, 2017.
- [53] C. Huang, X. Wang, J. Cao, S. Wang, and Y. Zhang, “Hcf: a hybrid cnn framework for behavior detection of distracted drivers,” *IEEE access*, vol. 8, pp. 109 335–109 349, 2020.
- [54] H. M. Eraqi, Y. Abouelnaga, M. H. Saad, M. N. Moustafa *et al.*, “Driver distraction identification with an ensemble of convolutional neural networks,” *Journal of Advanced Transportation*, vol. 2019, 2019.
- [55] K. Simonyan and A. Zisserman, “Two-stream convolutional networks for action recognition in videos,” *Advances in neural information processing systems*, vol. 27, 2014.
- [56] C. Feichtenhofer, A. Pinz, and A. Zisserman, “Convolutional two-stream network fusion for video action recognition,” in *Proceedings of the IEEE conference on Computer Vision and Pattern Recognition*, 2016, pp. 1933–1941.
- [57] A. Arnab, M. Dehghani, G. Heigold, C. Sun, M. Lucic, and C. Schmid, “Vivit: A video vision transformer,” in *2021 IEEE/CVF International Conference on Computer Vision (ICCV)*. Los Alamitos, CA, USA: IEEE Computer Society, oct 2021, pp. 6816–6826.
- [58] H. Fan, B. Xiong, K. Mangalam, Y. Li, Z. Yan, J. Malik, and C. Feichtenhofer, “Multiscale vision transformers,” in *Proceedings of the IEEE/CVF International Conference on Computer Vision*, 2021, pp. 6824–6835.
- [59] G. Bertasius, H. Wang, and L. Torresani, “Is space-time attention all you need for video understanding?” in *ICML*, vol. 2, no. 3, 2021, p. 4.
- [60] Z. Liu, J. Ning, Y. Cao, Y. Wei, Z. Zhang, S. Lin, and H. Hu, “Video swin transformer,” in *Proceedings of the IEEE/CVF conference on computer vision and pattern recognition*, 2022, pp. 3202–3211.
- [61] D. Bose, R. Hebbar, K. Somandepalli, H. Zhang, Y. Cui, K. Cole-McLaughlin, H. Wang, and S. Narayanan, “Movieclip: Visual scene recognition in movies,” in *2023 IEEE/CVF Winter Conference on Applications of Computer Vision (WACV)*, 2023, pp. 2082–2091.
- [62] A. Miech, D. Zhukov, J.-B. Alayrac, M. Tapaswi, I. Laptev, and J. Sivic, “Howto100m: Learning a text-video embedding by watching hundred million narrated video clips,” in *Proceedings of the IEEE/CVF International Conference on Computer Vision*, 2019, pp. 2630–2640.
- [63] N. C. Mithun, R. Panda, E. E. Papalexakis, and A. K. Roy-Chowdhury, “Webly supervised joint embedding for cross-modal image-text retrieval,” in *Proceedings of the 26th ACM international conference on Multimedia*, 2018, pp. 1856–1864.
- [64] J. Dong, X. Li, C. Xu, S. Ji, Y. He, G. Yang, and X. Wang, “Dual encoding for zero-example video retrieval,” in *Proceedings of the IEEE/CVF conference on computer vision and pattern recognition*, 2019, pp. 9346–9355.
- [65] M. S. Rahman, A. Venkatachalapathy, A. Sharma, J. Wang, S. V. Gursoy, D. Anastasiu, and S. Wang, “Synthetic distracted driving (syndd1) dataset for analyzing distracted behaviors and various gaze zones of a driver,” *Data in Brief*, vol. 46, p. 108793, 2023. [Online]. Available: <https://www.sciencedirect.com/science/article/pii/S2352340922009969>
- [66] “Kaggle. state farm distracted driver detection.” [Online]. Available: <https://www.kaggle.com/competitions/state-farm-distracted-driver-detection/data>
- [67] A. Miech, J.-B. Alayrac, L. Smaira, I. Laptev, J. Sivic, and A. Zisserman, “End-to-end learning of visual representations from uncurated instructional videos,” in *Proceedings of the IEEE/CVF Conference on Computer Vision and Pattern Recognition*, 2020, pp. 9879–9889.
- [68] D. P. Kingma and J. Ba, “Adam: A method for stochastic optimization,” *arXiv preprint arXiv:1412.6980*, 2014.
- [69] W. Zhou, Y. Qian, Z. Jie, and L. Ma, “Multi view action recognition for distracted driver behavior localization,” in *2023 IEEE/CVF Conference on Computer Vision and Pattern Recognition Workshops (CVPRW)*, 2023, pp. 5375–5380.
- [70] A. Roitberg, K. Peng, D. Schneider, K. Yang, M. Koulakis, M. Martinez, and R. Stiefelhagen, “Is my driver observation model overconfident? input-guided calibration networks for reliable and interpretable confidence estimates,” *IEEE Transactions on Intelligent Transportation Systems*, vol. 23, no. 12, pp. 25 271–25 286, 2022.



Md Zahid Hasan received his B.S. degree in Electrical and Electronic Engineering from Bangladesh University of Engineering and Technology in 2018. He is currently pursuing his Ph.D. in Electrical Engineering with the Department of Electrical and Computer Engineering at Iowa State University, IA. His research interests include Vision-Language models, computer vision, machine learning and decentralized deep learning.



Jiajing Chen received the B.S. degree in mechanical engineering from WuHan Institute of Technology, Wuhan, China in 2017 and M.S. degree in mechanical engineering from Syracuse University, Syracuse, NY, USA in 2019. He is currently pursuing the Ph.D. degree with the Department of Electrical Engineering and Computer Science, Syracuse University. His research interests include Point Cloud Segmentation, Weakly Supervised Object Detection and Few-shot Learning.



Jiyang Wang received his Bachelor's degree in electrical engineering from Anhui University of Science and Technology in 2017 and a Master's degree in electrical engineering from Syracuse University in 2019. He is currently a Ph.D. student in Electrical and Computer Engineering at Syracuse University. His research interests include computer vision, deep learning and human computer interaction.



Mohammed Shaiqur Rahman received his B.E. in Computer Science and Engineering from the National Institute of Engineering, India, in 2011. Then he joined IBM India Pvt Ltd and worked as a system engineer until early 2016. Later he joined the Department of Computer Science at Iowa State University, IA, where he completed his master's degree, and he is currently pursuing his Ph.D. His research interests include Artificial Intelligence, Machine Learning, Computer Vision, and Federated Learning.



Ameya Joshi received his B.S. degree in Electrical and Electronics Engineering from BITS Pilani, Goa, India in 2014. He is currently pursuing his Ph.D. in Electrical Engineering with the Department of Electrical and Computer Engineering at New York University. He was previously a Ph.D. student at Iowa State University (2018-2019) before going to NYU. His research interests include robust algorithms for multimodal models, adversarial robustness for deep learning, Vision-Text models, generative models for structured data, Physics Informed Generative models, Generative Adversarial Networks and computer vision.



Senem Velipasalar (M'04–SM'14) received the Ph.D. and M.A degrees in electrical engineering from Princeton University, Princeton, NJ, USA, in 2007 and 2004, respectively, the M.S. degree in electrical sciences and computer engineering from Brown University, Providence, RI, USA, in 2001, and the B.S. degree in electrical and electronic engineering from Bogazici University, Istanbul, Turkey, in 1999. From 2007 to 2011, she was an Assistant Professor at the Department of Electrical Engineering, University of Nebraska-Lincoln. She is currently

a Professor in the Department of Electrical Engineering and Computer Science, Syracuse University. The focus of her research has been on machine learning, mobile camera applications, wireless embedded smart cameras, multicamera tracking and surveillance systems.



Chinmay Hegde received his Ph.D. and M.S. in Electrical and Computer Engineering from Rice University in 2012 and 2010 respectively. He joined New York University, Tandon School of Engineering as an Assistant Professor in 2019. Previously, he was an Assistant Professor in the Department of Electrical and Computer Engineering at Iowa State University from 2015 to 2019. Prior to joining Iowa State, he was a postdoctoral associate in the Theory of Computation group at MIT from 2012 to 2015. His research focuses on developing principled, fast, and robust algorithms for diverse problems in machine learning, with applications to imaging and computer vision, materials design and transportation.



Anuj Sharma received his Ph.D. degree in Civil Engineering from Purdue University in 2008, and his M.S. degree in Civil Engineering from Texas A&M University in 2004. He was an Assistant Professor in the Department of Civil Engineering at the University of Nebraska-Lincoln. He is currently a Pitts-Des Moines Inc. Professor in Civil Engineering at Iowa State University. His research focuses on traffic operations, big data analytics, machine learning, and traffic safety.



Soumik Sarkar received his Ph.D. in Mechanical Engineering from Penn State University in 2011. He joined the Department of Mechanical Engineering at Iowa State as an Assistant Professor in Fall 2014. Previously, he was with the Decision Support and Machine Intelligence group at the United Technologies Research Center for 3 years as a Senior Scientist. He is currently a Professor of Mechanical Engineering and Walter W Wilson Faculty Fellow in Engineering at Iowa State University. He also serves as the Director of Translational AI Center at Iowa State. His research focuses on machine learning, and controls for Cyber-Physical Systems applications such as aerospace, energy, transportation, manufacturing and agricultural systems.